Structural Studies on Supramolecular Adducts of Cyclodextrins with the Complex [Ru([9]aneS$_3$)(bpy)Cl]Cl

Joana Marques, Lucia Anjo, Maria P.M. Marques, Teresa M. Santos, Filipe A. Almeida Paz, Susana S. Braga

PII: S0022-328X(08)00384-7
DOI: 10.1016/j.jorganchem.2008.06.023
Reference: JOM 15536

To appear in: *Journal of Organometallic Chemistry*

Received Date: 23 April 2008
Revised Date: 16 June 2008
Accepted Date: 18 June 2008

Please cite this article as: J. Marques, L. Anjo, M.P.M. Marques, T.M. Santos, F.A. Almeida Paz, S.S. Braga, Structural Studies on Supramolecular Adducts of Cyclodextrins with the Complex [Ru([9]aneS$_3$)(bpy)Cl]Cl, *Journal of Organometallic Chemistry* (2008), doi: 10.1016/j.jorganchem.2008.06.023

Manuscript for *J. Organomet. Chem.* 23/06/2008

Structural Studies on Supramolecular Adducts of Cyclodextrins with the Complex [Ru([9]aneS$_3$)(bpy)Cl]Cl

Joana Marques,[a] Lucia Anjo,[a] Maria P. M. Marques,[b] Teresa M. Santos,[a] Filipe A. Almeida Paz,[a] and Susana S. Braga *[a]

[a] Department of Chemistry, CICECO, University of Aveiro, 3810-193 Aveiro, Portugal
Fax: (internat.) + 351-234-370084
E-mail: sbraga@ua.pt

[b] Science and Technology Faculty, Molecular Physical Chemistry Research Group, Department of Chemistry, University of Coimbra, Apt. 3126, 3001-401 Coimbra, Portugal

Keywords: Cyclodextrins / Inclusion compounds / Ruthenium complexes / Powder X-ray Diffraction /

The complex [Ru([9]aneS$_3$)(bpy)Cl]Cl (bpy = 2,2´-bipyridine) was immobilised in plain β-cyclodextrin (β-CD) and permethylated β-CD (TRIMEB) to yield two adducts with a 1:1 host:guest stoichiometry. The adducts were studied by powder X-ray diffraction (XRD), thermogravimetric analysis (TGA), $^{13}C\{^1H\}$ CP/MAS NMR and vibrational spectroscopy (FT-IR and Raman). Results support the formation of stable supramolecular adducts with a proposed geometry in which the coordinated bypiridine fragment of the guest is partially included in the host cavities, and the bulky [9]aneS$_3$ fragment protrudes out to the interstitial spaces. A packing mode is proposed for [Ru([9]aneS$_3$)(bpy)Cl]Cl·TRIMEB, obtained by Monte Carlo optimisation of the XRD data. TRIMEB molecules are stacked in tilted channels, with the voluminous part of the guest molecules in the inter-channel space. The behaviour of [Ru([9]aneS$_3$])(bpy)Cl]Cl upon CD encapsulation and the chloride ligand hydrolysis process in solution for all compounds were studied in detail by Raman spectroscopy.

---

1. Introduction

Cyclodextrins (CDs) are water soluble cyclic oligosaccharides capable of forming inclusion compounds with a wide range of organic molecules, inorganic ions and metallo-organic species [1-3]. Suitable guests include transition-metal complexes and organometallic compounds bearing hydrophobic ligands such as cyclopentadienyl (Cp = η^5-C_5H_5) and η^6-arene groups [4-6], capable of docking into the host cavity by non-covalent bonding (either van der Waals or charge-transfer interactions). We have explored the protecting and bio-delivery properties of these hosts to enhance the activity of antitumour metal compounds such as ferrocene derivatives [7] and metallocene dihalides, in particular Cp_2MCl_2 (Cp = cyclopentadienyl, M = Nb, Mo) [8-10]. In particular, cytotoxic assays carried out for pure and included molybdenocene dichloride showed a higher activity upon encapsulation, in particular when using permethylated β-cyclodextrin (TRIMEB) [9]. We have also used cyclodextrin encapsulation to modulate the activity of carbonyl organometallics such as $CpFe(CO)_2X$ (X = Cl, CN) [11-13], Cp'Mo(η^3-C_3H_5)$(CO)_2$ [14], $CpMo(LL)(CO)_2$ (L = 2 × CH_3CN or LL = 2,2'-*bis*-imidazole) [15] and $CpMo(CO)_3CH_2CONH_2$ [16]. The latter compound was revealed to be a useful catalyst with a wide range of applications modulated by the host: whilst the β-CD inclusion compound is suitable for heterogeneous solid–liquid systems, the TRIMEB inclusion compound is instead more suited to homogeneous or liquid–liquid biphasic systems.

Our most recent work is focused on the application of ruthenium complexes as cytotoxic agents. For this purpose, some of us have developed a series of Ru(II) complexes with the face-capping ligand trithyacyclononane ([9]aneS_3) and planar aromatic amines suitable for DNA intercalation [17]. The crystal structures of these compounds were found to be largely stabilised by hydrogen bonding interactions and the coordinated planar aromatic amines exhibit π-stacking arrangements which mimic the structure of polypyridyl complexes intercalated with DNA. The intercalative properties of some of these compounds have also been demonstrated by UV/Vis titration studies, in particular for [Ru([9]aneS_3)dppzCl]Cl (dppz = dipyrido[3,2a:2',3'c]phenazine) [18]. Following the strategy of molecular encapsulation that allowed us to improve the cytotoxic properties of molybdenocene dichloride [4b], here we wish to report the first supramolecular adducts of the trithyacyclononane-Ru(II) guest [Ru([9]aneS_3)(bpy)Cl]Cl (bpy = 2,2´-bipyridine) with the cyclodextrin hosts β-CD and 2,3,6-tri-*O*-methyl-β-CD (TRIMEB).

2. Experimental

2.1.General remarks

β-CD was kindly donated by laboratoires La Roquette (France), and heptakis-2,3,6-tri-*O*-methyl-β-CD was obtained from Cyclolab. All air-sensitive operations were carried out using standard Schlenk techniques under nitrogen. Solvents were dried by standard procedures, distilled under nitrogen or argon, and kept over 4 Å molecular sieves.

Microanalyses for CHN were performed at the University of Cambridge (Department of Chemistry) on an Exeter Analytical CE 440 Elemental Analyser. Samples were combusted under an oxygen atmosphere at 975°C for 1 minute, and helium used as purge gas. The ruthenium content was determined by ICP-OES analyses at the Central Laboratory for Analysis, University of Aveiro (by L. Soares).

TGA studies were carried out using a Shimadzu TGA-50 system at a heating rate of 5 ºC min^{-1} under air.

Powder X-ray diffraction data were collected at ambient temperature on an X'Pert MPD Philips diffractometer (Cu K_α X-radiation, $\lambda = 1.54060$ Å), equipped with an X'Celerator detector, a curved graphite-monochromated radiation and a flat-plate sample holder, in a Bragg-Brentano para-focusing optics configuration (40 kV, 50 mA). Intensity data were collected in continuous scanning mode in the *ca.* $4 \leq 2\theta^o \leq 70$ angular range.

FT-IR spectra were recorded on a Unican Mattson Mod 7000 FTIR spectrophotometer.

$^{13}C\{^1H\}$ CP/MAS NMR spectra were recorded at 125.72 MHz on a (11.7 T) Bruker Avance 500 spectrometer, with an optimised π/2 pulse for ^1H of 4.5 μs, 2 ms contact time, a spinning rate of 7 kHz and 12 s recycle delays. Chemical shifts are quoted in parts per million from tetramethylsilane.

*2.2. Preparation of [Ru([9]aneS₃)(bpy)Cl]Cl (**1**)*

This compound was prepared as described in the literature [19].

FT-IR (KBr, cm^{-1}): nu(tilde) = 3529 s, 3434 vs, 3355 vs, 3061 m, 2975 m, 2931 m, 2075 m, 1642 s, 1622 sh, 1599 s, 1470 s, 1443 s, 1411 s, 1314 m, 1274 m, 1240 m, 1221 w, 1160 m, 1107 m, 1016 w, 961 w, 911 m, 823 m, 766 vs, 761 vs, 747 sh, 730 s, 706 m, 676 w, 647 w, 567 m, 540 m, 473 w, 425 w. $^{13}C\{^1H\}$ CP/MAS NMR: δ = 156.8, 155.2 (bpy C*a*, see carbon labelling scheme below), 152.4 (bpy C*e*), 135.0, 140.0 (bpy C*c*), 127.8, 126.8 (bpy C*d*), 122.8 (bpy, C*b*), 39.8, 38.7, 36.5, 31.5, 29.7, 28.8 ppm (all [9]aneS₃).

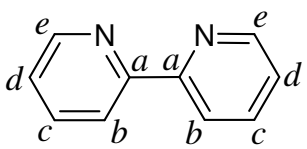

*2.3. Preparation of [Ru([9]aneS₃)(bpy)Cl]Cl·β-CD (**2**)*

A solution of β-CD (47.3 mg, 0.036 mmol) in water (10 cm^3) at 25 ºC was treated dropwise with a solution of [Ru([9]aneS_3)(bpy)Cl]Cl (**1**) (18.4 mg, 0.036 mmol) in acetonitrile (10 cm^3), and the resultant orange solution was stirred for 20 min at 25 ºC and then immediately frozen using liquid nitrogen. After solvent removal by freeze-drying, a pale orange voluminous powder was obtained. Anal. Calcd for $(C_{42}H_{70}O_{35})\cdot(C_{16}N_2H_{20}S_3RuCl_2)\cdot 10H_2O$ (1858.4) C, 38.20; N, 1.54; H, 6.08%. Found: C, 37.92; N 1.35; H, 7.00%. TGA up to 78 °C revealed a sample weight loss of 8.6% (calcd: for loss of $9H_2O$, 8.8%).

FT-IR (KBr, cm^{-1}): nu(tilde) = 3387 vs, 2927 m, 1636 m, 1604 sh, 1465 sh, 1445 m, 1412 m, 1384 m, 1334 m, 1300 m, 1242 m, 1202 m, 1156 s, 1098 sh, 1078 s, 1029 vs, 1002 s, 946 m, 937 m, 911 w, 888 w, 859 m, 824 w, 762 m, 722 w, 706 m, 647 vw, 609 m, 581 m, 531 m, 480 vw, 447 vw, 358 w, 302 m. $^{13}C\{^1H\}$ CP/MAS NMR: δ = 155.1, 152.6, 144.2, 140.0, 128.3, 123.8 (guest, bipyridine), 103.0 (β-CD, C1 – see numbering scheme below), 82.4 (β-CD, C4), 73.0 (β-CD, C2,3,5), 60.8 ppm (β-CD, C6), 36.7, 31.6 (guest, [9]aneS_3).

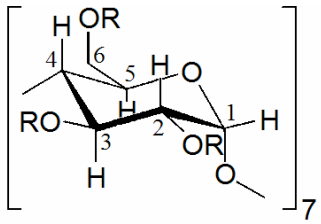

R = H (β-CD)
R = Me (TRIMEB)

*2.4. Preparation of [Ru([9]aneS_3)(bpy)Cl]Cl·TRIMEB (**3**)*

A solution of TRIMEB (143.0 mg, 0.10 mmol) in ethanol (5 cm^3) was treated stepwise with solid [Ru([9]aneS_3)(bpy)Cl]Cl (**1**) (50.8 mg, 0.10 mmol) and stirred for 1 h. The solution was then evaporated to dryness, giving an orange solid. Anal. Calcd for **3** $(C_{63}H_{112}O_{35})\cdot(C_{16}N_2H_{20}S_3RuCl_2)\cdot 6H_2O$ (2010.7): C, 47.19; N, 1.39; H, 7.22; Ru, 5.03. Found: C, 47.13; N, 1.14; H, 6.68; Ru, 5.22%.

FTIR (KBr, cm^{-1}): nu(tilde) = 3442 s, 3066 m, 2984 s, 2939 s, 2833 m, 1733 m, 1623 m, 1600 m, 1558 w, 1541 w, 1464 m, 1446 m, 1403 sh, 1384 s, 1322 m, 1306 m, 1270 m, 1232 sh, 1195 s, 1165 vs, 1142 vs, 1108 vs, 1089 vs, 1068 vs, 1038 vs, 973 s, 954 m, 909 m, 857 m, 827 m, 806 w, 772 s, 731 m, 705 m, 668 m, 554 m, 4217 m, 399 w, 350 w, 340 w. $^{13}C\{^1H\}$ CP/MAS NMR: δ = 155.2, 151.4, 140.6, 138.2, 129.0 (guest, bipyridine), 99.8 (TRIMEB, C1), 83.1 (TRIMEB, C2,3,4), 71.6 (TRIMEB, C5,6), 58.8 ppm (TRIMEB, O–CH_3), 39.2, 36.7, 30.6 (guest, [9]aneS_3).

2.5. Hydrolytic studies in solution

Hydrolysis of the Ru–Cl bond in the complex ion [Ru([9]aneS_3])(bpy)$Cl]^+$ was monitored in solution (at concentrations between 5 and 10 $mmol.dm^{-3}$) by Raman spectroscopy, both aqueous and in physiological serum ($[Cl^-]$ = 0.9% *(w/v)*= 154 $mmol.dm^{-3}$).

Raman spectra were obtained for the solutions, at room temperature, in a triple monochromator Jobin-Yvon T64000 Raman system (focal distance 0.640 m, aperture *f*/7.5) with holographic gratings of 1800 grooves.mm^{-1}. The premonochromator stage was used in the subtractive mode. The detection system was a liquid nitrogen cooled non-intensified 1024×256 pixel (1") Charge Coupled Device (CCD). The entrance slit was set to 200 μm, and the slit between the premonochromator and the spectrograph was opened to 12 mm.

The excitation radiation was provided (*ca.* 120 mW at the sample position) by the 514.5 nm line of an Ar^+ laser (Coherent, model Innova 300). A 90º geometry between the incident radiation and the collecting system was employed. Samples were sealed in Kimax glass capillary tubes of 0.8 mm inner diameter. Under the above mentioned conditions, the error in wavenumbers was estimated to be within 1 cm^{-1}.

3. Results and Discussion

Preparation of the inclusion compounds with the guest salt [Ru([9]aneS$_3$)(bpy)Cl]Cl (**1**) was carried out using a minimal amount of water as the solvent so to avoid the decomposition of the metallic complex due to chloride hydrolysis. In the case of TRIMEB, co-dissolution in ethanol was the process of choice. This "water-free" inclusion process developed by us for methylated cyclodextrins was revealed to be quite suitable for guests that are unstable in water [20,21]. For the dissolution of β-CD water is required, thus a short time of reaction (20 minutes) was used to prevent chloride hydrolysis. Elemental analysis of compounds [Ru([9]aneS$_3$)(bpy)Cl]Cl·β-CD (**2**) and [Ru([9]aneS$_3$)(bpy)Cl]Cl·TRIMEB **(3**) confirmed the expected 1:1 host:guest molar ratio for the final products.

Preliminary structural investigations using X-ray diffraction data allowed an immediate confirmation of the presence of true inclusion compounds of cyclodextrins because the collected patterns for **2** and **3** are markedly distinct from those obtained by the superimposition of the diffractograms of the pure host and guest components [2]. In the case of adduct **2**, although the overall pattern reveals a low crystallinity, one may find a few broad reflections centred at 4.4, 8.9, 10.6, 12.5 and 17.6 2θº that do not match those of neither of the components (β-CD or **1**); the same can be observed for adduct **3**, as shown in Figure 1.

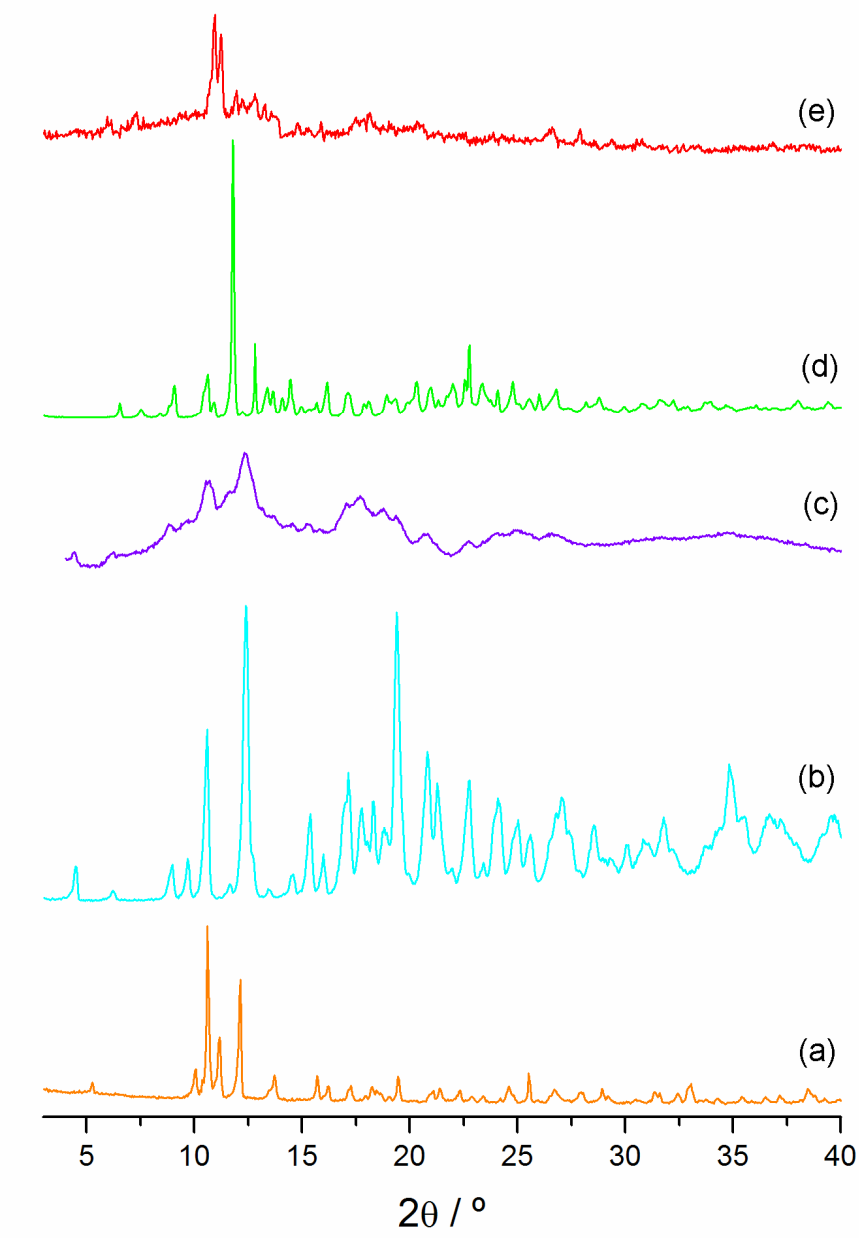

Figure 1 – Powder XRD patterns of (a) [Ru([9]aneS$_3$)(bpy)Cl]Cl (**1**), (b) β-CD hydrate, (c) the adduct [Ru([9]aneS$_3$)(bpy)Cl]Cl·β-CD (**2**), (d) TRIMEB and (e) the adduct [Ru([9]aneS$_3$)(bpy)Cl]Cl·TRIMEB (**3**).

The features of the powder patterns for **2** and **3** are also markedly typical [8,12], namely the presence of low-resolved reflection lines at low angle, a significant background, and low-intensity or even indiscernible reflections at high angles. Noteworthy, the low crystallinity of the samples seems to be directly related with the geometrical features of the included species. Indeed, the relatively large size of the cationic [Ru([9]aneS$_3$)(bpy)Cl] $^+$ complex possibly induces a considerable structural disorder in the solid-state packing of the host and guest chemical species. This feature, allied with the inherent thermal disorder associated with the water molecules of crystallisation and the structural flexibility of the cyclodextrin rings, most likely leads to the isolation of materials with low long-range order.

Despite the very low overall crystallinity of the sample, the experimental powder X-ray diffraction

pattern of [Ru([9]aneS$_3$)(bpy)Cl]Cl·β-CD (**2**) could be indexed with DICVOL04 [22] (fixed absolute error on each line of 0.03º 2θ; no impurity lines were allowed) using the first 18 more intense and better resolved reflections (located using the derivative-based peak search algorithm provided with Fullprof.2k) [23,24]. Systematic absences for an initially-calculated monoclinic unit cell were inspected using CHECKCELL [25], which indicated space group $P2_1$ as the most suitable to define the overall symmetry of the material. A Le Bail whole-powder-diffraction-pattern profile decomposition [26] using fixed (and manually selected) background points produced a reasonably good fitting (R_{Bragg} = 0.48% and χ^2 = 1.90 – see Figure S1 in the Electronic Supporting Information) with the unit cell parameters of this inclusion compound converging to: a = 20.72(1) Å, b = 10.296(6) Å, c = 15.096(7) Å and β = 109.05(5) Å (M_{18} = 10.4 [27], and F_{18} = 15.2 [28]). A search in the literature revealed a single known and closely related material recently reported by the research groups of Kurokawa & Ishida in which [$CuCl_2(H_2O)_2$] complexes co-crystallise with β-CD [29]. It is interesting to emphasise that in this previously-reported material the copper(II) complexes are not included inside the hydrophobic cavities of the cyclodextrin, sitting instead at the bottom of the host. Comparing the total volumes for the unit cells [*ca.* 3033 and 3044 Å^3 for [$CuCl_2(H_2O)_2$]·β-CD and **2**, respectively] it is thus feasible to assume that in **2** the guest complex are most likely included inside the cavity of the host. Moreover, there is a small increase in the length of the *c*-axis, which is also coherent with a small increase in the spatial separation between β-CDs most likely due to the presence of bulky ruthenium(II) complexes. The poor quality of the diffractogram for compound **2** did not allow any further structural studies.

Compound [Ru([9]aneS$_3$)(bpy)Cl]Cl·TRIMEB (**3**) is significantly more crystalline, as clearly depicted in Figure 2. Indexing of the powder X-ray diffraction pattern and analysis of the systematic absences were performed by adopting a similar strategy to that described for the previous compound and using in tandem the software packages DICVOL04, Fullprof.2k and CHECKCELL. It is important to stress that a plausible initial monoclinic indexing could only be computed, and having reasonable figures of merit (M_{14} = 12.1, and F_{14} = 35.8), when the presence of one or more impurity lines was allowed. Indeed, solutions which account for all the initial (and better resolved) reflections selected from the powder pattern, further assuming a peak position error of ±0.03º, could only be derived using the TREOR90 algorithm [30] with all belonging to the triclinic crystal system. As revealed by a search in the Cambridge Structural Database (CSD, Version 5.29 – November 2007) [31,32] there is not a single known report of a triclinic unit cell containing TRIMEB molecules. Moreover, further structural studies by assuming these triclinic unit cell solutions in FOX [33,34] did not lead to better structural models and, consequently, these triclinic solutions were discarded. The monoclinic solution was refined in space group $P2_1$ by employing a Le Bail whole-powder-diffraction-pattern profile decomposition (fixed background points were manually selected from the powder pattern): a = 19.295(4) Å, b = 16.664(3) Å, c = 15.426(3) Å and β = 104.224(9) Å (R_{Bragg} = 1.28% and χ^2 = 9.75 – see Figure S2 in the Electronic Supporting Information).

A plausible structural model derived from powder X-ray data for [Ru([9]aneS$_3$)(bpy)Cl]Cl·TRIMEB (**3**) was calculated using the software package FOX [33,34] and by adopting the general principles previously described by us for related materials [8,12]. This systematic strategy probes all possible structural orientations in direct space of the selected chemical entities (which are treated as rigid bodies), thus leading to the selection of the most chemically-feasible structural model for the compound in study. The geometrical parameters for the TRIMEB cyclodextrin were extracted from the first adduct with an organometallic guest [CpFe(CO)$_2$Cl], fully characterised by single-crystal X-ray diffraction and recently reported by us [11]. For the guest molecular entity, [Ru([9]aneS$_3$)(bpy)Cl]$^+$, a search in the CSD reveals only two known crystallographic reports in which this cation co-crystallises with Cl$^-$/H$_2$O (CSD refcode RIFMOI) [19] or trifluorosulfonate anions (CSD refcode YAVNIT) [35]. Because the geometrical features for [Ru([9]aneS$_3$)(bpy)Cl]$^+$ do not change considerably for different counter-ions, and also because we have employed the chloride salt for the preparation of compound **3**, the molecular geometry of RIFMOI was selected for further studies. The host and guest molecules were transformed into Fenske-Hall *Z*-matrices calculated using BABEL (hydrogen atoms have been removed in order or simplify the calculations) [36]. For the cationic [Ru([9]aneS$_3$)(bpy)Cl]$^+$ complex (guest) the central ruthenium atom was selected as the pivot atom which greatly facilitates the mobility of this molecular unit during the optimisation process.

Monte Carlo optimisations (using the optimised parallel tempering algorithm) were launched in FOX [33,34] with the three individual mathematical objects (the TRIMEB host, the guest ruthenium(II) cationic complex and a charge-balancing chloride anion) having the parameters of the *Z*-matrices fixed (*i.e.*, each entity was treated as a rigid body and only optimisation of the relative orientation and crystallographic position inside the unit cell were allowed). The water molecules of crystallisation, whose content was unequivocally determined from elemental composition and thermoanalytical studies (see Experimental Section and the following paragraphs for discussion of the results), were not included in the Monte Carlo optimisation for simplicity. Due to the use of antibump restraints to facilitate the optimisation process and to lead more rapidly to chemically-feasible models, the terminal methyl groups of TRIMEB were manually removed from the FHZ matrix imported into FOX. It is important to emphasise that this strategy is chemically- and computationally-feasible since it reduces steric hindrance between neighbouring molecules and also minimises (but not removes) the occurrence of overlapping atoms which, in the real crystal structure, do not exist due to the conformational flexibility of TRIMEB.

After full Monte Carlo convergence, the systematic permutation in $P2_1$ of the three chemical entities led to a structural model whose simulated powder X-ray diffraction pattern compares relatively well with the experimental one (calculated weighted residual of $R_{wp} = 0.087$) (Figure 1). Fractional atomic coordinates and a CIF file for the hypothetical structural model are supplied as Electronic Supporting Information. These structural studies clearly demonstrate that the cationic [Ru([9]aneS$_3$)(bpy)Cl]$^+$ guest complex is not fully included inside the cavity of the TRIMEB host (Figure

2), most likely due to its relatively large size. The cations are instead regularly distributed in-between the TRIMEB hosts, occupying the intermolecular void spaces (Figure 2) and in relatively close proximity with the charge-balancing Cl^- anion. This structural feature, despite unusual, is not unprecedented for cyclodextrin inclusion compounds and was for example reported by K. Harata for the DIMEB complexes with *p*-iodophenol and *p*-nitrophenol [37]. Nevertheless, it is of considerable importance to stress that the packing features of TRIMEB are still typical with the formation of tilted channels in the hypothetical structural model running parallel to the *c*-axis of the unit cell (Figure 3). The larger tilting angle can be associated with the presence of the bulky ruthenium(II) complexes.

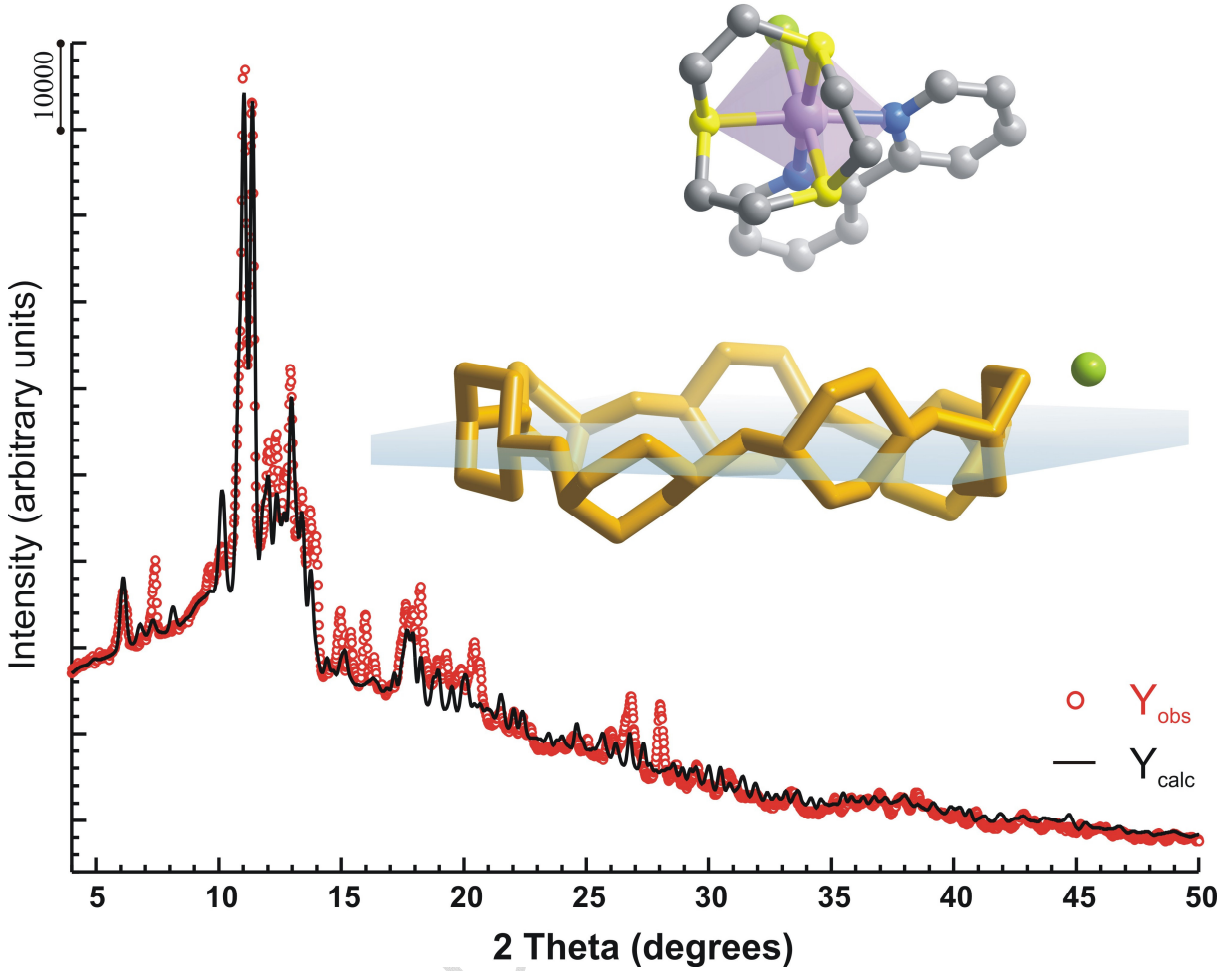

Figure 2 – (*Bottom*) Experimental data (red circles) and simulated using FOX (lower solid blue line) powder X-ray diffraction patterns for [Ru([9]aneS$_3$)(bpy)Cl]Cl·TRIMEB (**3**). (*Top*) Chemical moieties composing the asymmetric unit of the hypothetical structural model of compound **3**. The TRIMEB molecule was simplified for clarity purposes by a ring-shaped object solely composed by the seven α-D-glucopyranoside units.

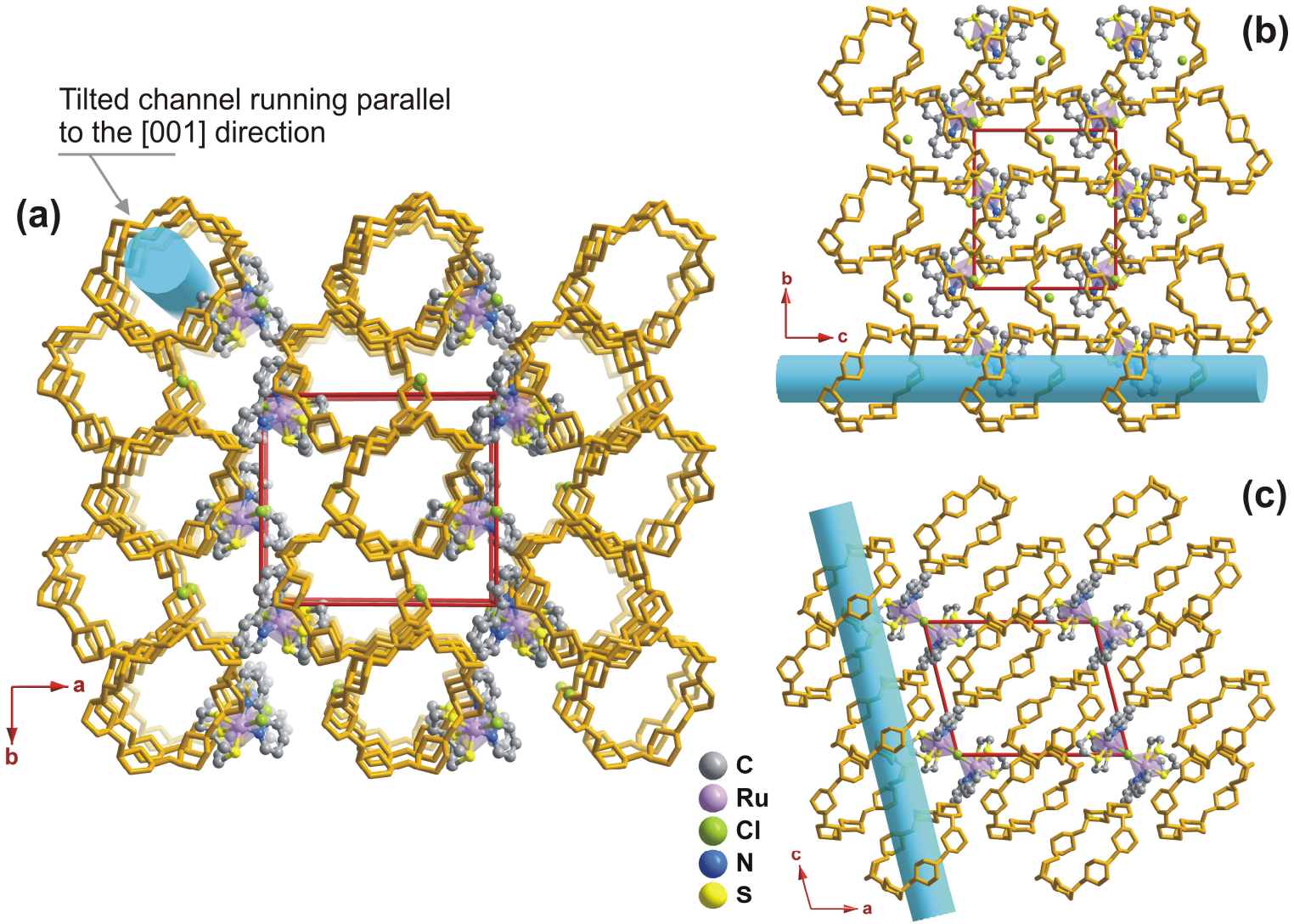

Figure 3 – Crystal packing of [Ru([9]aneS$_3$)(bpy)Cl]Cl·TRIMEB (**3**) viewed in perspective along the **(a)** [001], **(b)** [100] and **(c)** [010] directions of the unit cell, emphasising the tilted channel-type distribution of the cyclodextrin units. TRIMEB molecules have been simplified for clarity by ring-shaped objects composed by the seven α-D-glucopyranoside units. [Ru([9]aneS$_3$)(bpy)Cl]$^+$ cations and Cl$^-$ anions are drawn in mixed polyhedral and ball-and-stick modes.

Thermogravimetric analysis was also useful for the recognition of inclusion complex formation in compounds **2** and **3** (Figure 3). The adduct [Ru([9]aneS$_3$)(bpy)Cl]Cl·β-CD (**2**) exhibits a step from room temperature up to about 78 °C, assigned to the removal of water molecules located in the β-CD cavities and in the interstices in-between the macrocycles. The corresponding total weight loss is of *ca.* 8.6%, which indicates that the approximate number of water molecules per β-CD molecule is about 9. For comparison, plain β-CD hydrate shows a similar well-defined step from room temperature up to about 80 °C, with a mass loss of 14.6% (11 water molecules per β-CD molecule). The partial occupation of the β-CD cavities by the guests is usually accompanied by a reduction of hydration waters, thus supporting the assumption (from powder XRD data) that a new supramolecular structure was formed between β-CD and the guest [Ru([9]aneS$_3$)(bpy)Cl]Cl, involving a partial inclusion of the molecule. After the dehydration step, the TG curve for **2** features an early decomposition of the host (plain β-CD hydrate starts to decompose around 270 ºC). This difference is attributed to the promoting effects of the ruthenium complex on the decomposition of β-cyclodextrin, and is an evidence of a significant strong host-guest affinity [38].

[Ru([9]aneS$_3$)(bpy)Cl]Cl·TRIMEB (**3**) has an inverse behaviour. While pure TRIMEB starts to melt and decompose at about 175 ºC, compound **3** starts to decompose around 265 ºC. To further investigate this unusual feature we have prepared the 1:1 physical mixture of the two components by mechanical grinding (inset in Figure 3). Surprisingly, both the adduct and the physical mixture feature similar decomposition profiles. We also note that the residual masses at 550 ºC are similar and of about 7%, thus further supporting the 1:1 host-to-guest stoichiometry in the inclusion compound **3** as determined by microanalysis. The higher thermal stability of both [Ru([9]aneS$_3$)(bpy)Cl]Cl·TRIMEB (**3**) and its corresponding mix are an unusual feature, only observed when TRIMEB (rather than native β-CD) is used as host, and seems to occur with very specific guest types. We have previously registered this thermal decomposition profile for TRIMEB encapsulated metallocenes – Cp_2MoCl_2 [9] and Cp_2NbCl_2 [8] – and are currently obtaining similar results for other supramolecular TRIMEB adducts [39].

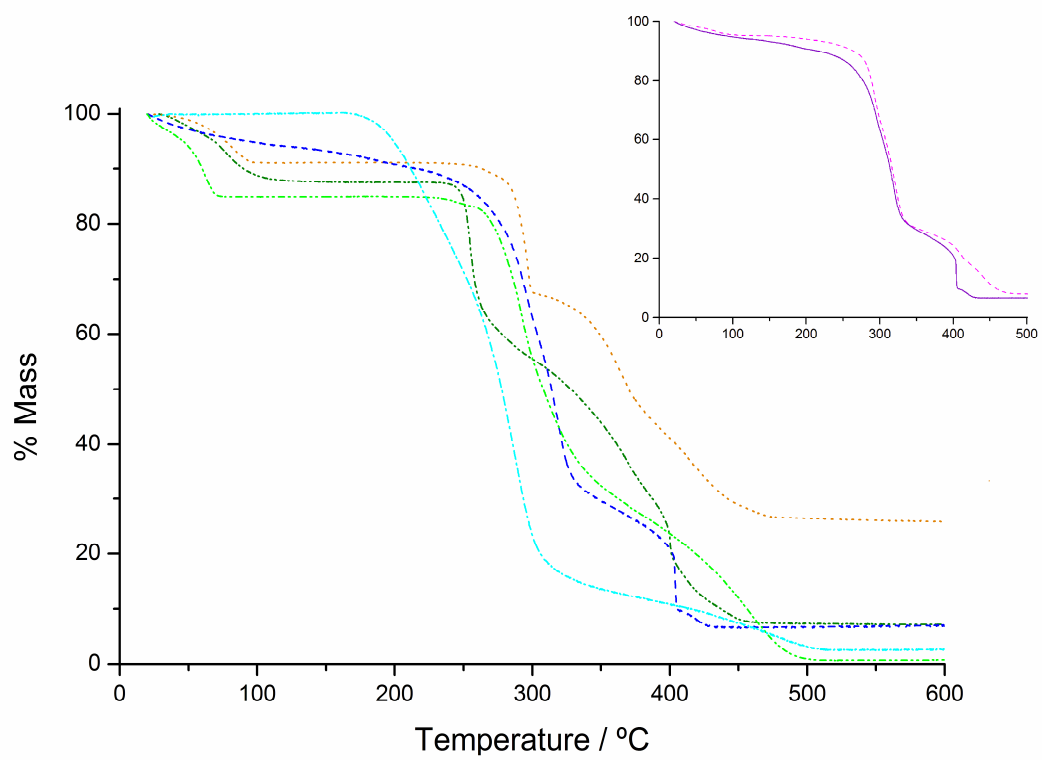

Figure 4 – Thermal decomposition profiles for [Ru([9]aneS$_3$)(bpy)Cl]Cl (**1**) (- - -), β-CD (·· – ·· –), [Ru([9]aneS$_3$)(bpy)Cl]Cl·β-CD (**2**) (- - – - - –), TRIMEB (– - – -) and [Ru([9]aneS$_3$)(bpy)Cl]Cl·TRIMEB (**3**) (– – –). The inset shows a comparison of the TG profile for compound **3** (solid, purple) with that of its corresponding physical 1:1 molar mixture (pink, dashed).

The $^{13}C\{^1H\}$ CP/MAS NMR spectra of the complex **1**, the hosts β-CD and TRIMEB and their corresponding inclusion compounds **2** and **3** are shown in Figure 4. Plain β-CD hydrate exhibits a complex $^{13}C\{^1H\}$ CP/MAS NMR spectrum with multiple sharp resonances for each type of carbon atom. These features have been correlated with different torsion angles about the α(1→4) linkages [40,41], and with torsion angles describing the orientation of the hydroxyl groups [42]. Upon inclusion to give [Ru([9]aneS$_3$)(bpy)Cl]Cl·β-CD (**2**) the resonances due to the C1, and C2,3,5 host carbon atoms appear as single broad peaks with maxima peaking at δ 102.3 and 72.8 ppm, respectively, with little or no structure. Moreover, resonances associated with carbon atoms C4 and C6 feature a reduction in multiplicity and structure. These observations may have been associated with symmetrisation of the β-CD macrocycle in order to better accommodate the guest molecules [8,10,12-15].

The complex **1** features multiple resonances for the thioether [9]aneS$_3$ ring grouped in two sets of triplets (from 42 to 25 ppm); this is in agreement with two possible different conformations for this ring, as postulated by solution studies by ^1H and ^{13}C NMR [19]. These authors proposed that the two possible conformations have Cs symmetry, with a plane of symmetry that runs through the Ru, the Cl, one sulfur atom and bisects the angle N—Ru—N of the bipyridine ligand. The guest carbon atom resonances are also observed in the spectrum of compound **2**, though featuring a dramatic loss of multiplicity. This way, resonances for the [9]aneS$_3$ carbons are reduced to two broad signals by β-CD inclusion and those of

bipyridine also feature line broadening, with only one broad signal for carbons *a* and *e*. This overall pattern may reflect a more symmetric environment around the guest as a result of its incorporation into the crystalline lattice of the inclusion compound.

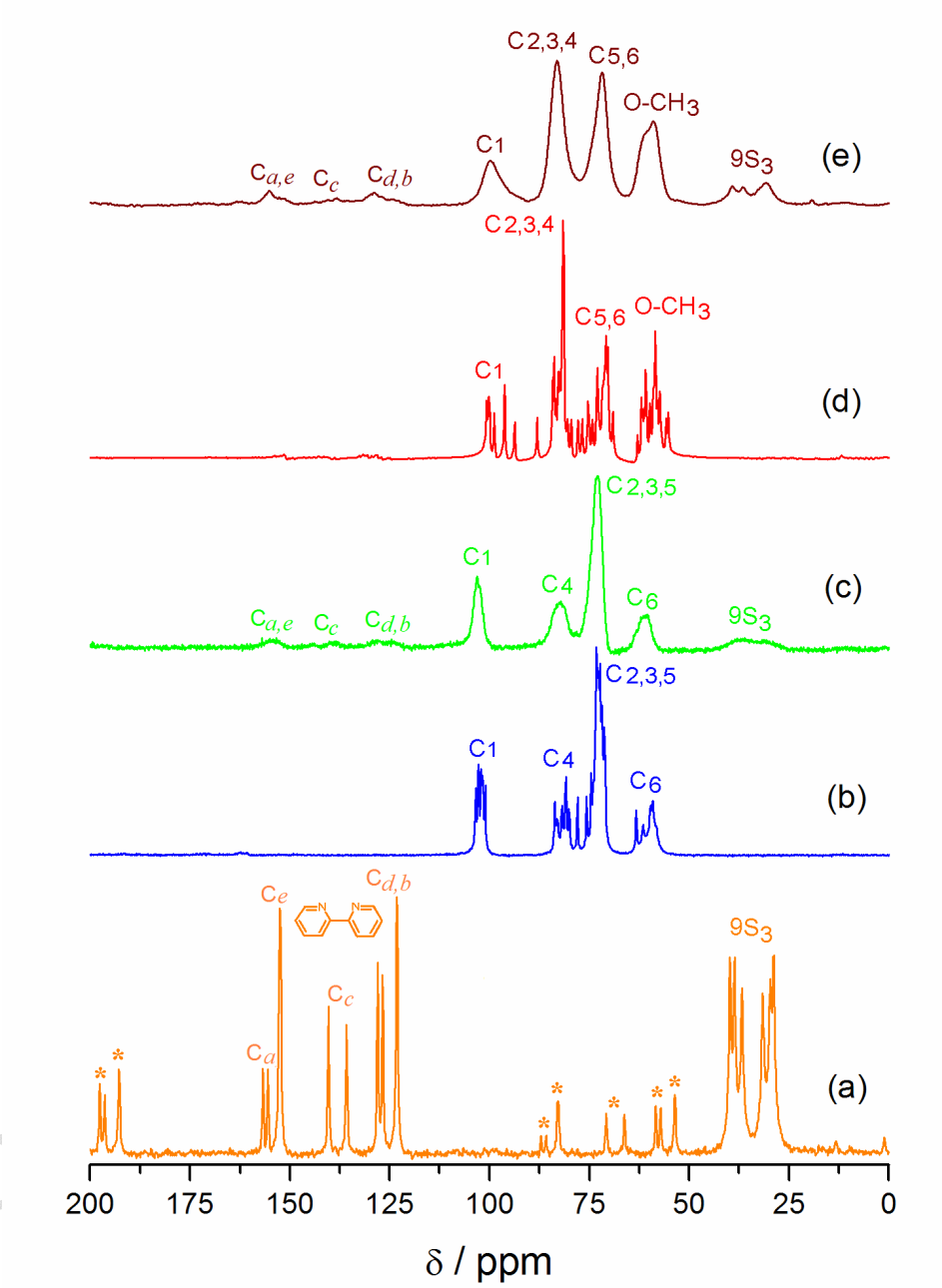

Figure 5 – Solid-state $^{13}C\{^{1}H\}$ CP/MAS NMR spectra of (a) [Ru([9]aneS$_3$])(bpy)Cl]Cl (**1**), (b) pure β-CD hydrate, (c) the inclusion compound [Ru([9]aneS$_3$])(bpy)Cl]Cl·β-CD (**2**), (d) TRIMEB and (e) the inclusion compound [Ru([9]aneS$_3$])(bpy)Cl]Cl·TRIMEB (**3**). 9S$_3$ represents the ligand [9]aneS$_3$ and spinning sidebands are denoted by asterisks. For the carbon labelling scheme of the cyclodextrins, of the guest ligand bipyridine and the complete listing of resonances, please refer to the experimental section.

Like plain β-CD hydrate, the $^{13}C\{^{1}H\}$ CP/MAS NMR spectrum of TRIMEB also shows multiple resonances for each type of carbon atom. This may be due to a collapsed conformation in the solid state by inversion of the conformation of one glucose unit to the $^{1}C_4$ conformation as observed for TRIMEB

monohydrate (form 1), or to an overall asymmetry in the local environment of the glucose units due to self inclusion of two primary methoxy groups from a neighbouring molecule, as found for the crystals of anhydrate TRIMEB (form 3) [43]. (Note that an unambiguous assignment of the herein used TRIMEB to the monohydrate or anhydrate forms from diffraction data could not be made due to the absence of reference data collected at room temperature.) The multiplicity is lost for the inclusion compound [Ru([9]aneS$_3$])(bpy)Cl]Cl·TRIMEB (**3**) and only broad peaks are observed, indicating a change in the conformation of the host macrocycle [20,21]. Note that at least two resonances are discernible for the methyl carbon atoms, indicating that these groups exist in different environments, as a result of the high flexibility of their bonds. Such kind of disorder of the primary methoxyl groups is quite common in the crystal lattices of TRIMEB inclusion compounds. The resonances for the guest molecule in **3** feature even further reduction in multiplicity than for the adduct **2**. In fact, only three broad resonances are found for the carbons of the [9]aneS$_3$ macrocycle and those of the bipyridine ligand have coalesced into four broad signals centred at δ 155.3, 140.2, 138.2 and 128.6 ppm.

The FT-IR spectrum of **1** shows the typical bipyridine bands with maxima peaking at $\bar{\nu}$ 1642, 1622, 1599 cm^{-1}. These appear as shoulders around 1604 and 1600 cm^{-1} upon inclusion in β-CD and TRIMEB, respectively (other bands are overlapped by the broad band associated with the deformation vibrational mode of the hydration water molecules, centred at 1636 and 1623 cm^{-1}, respectively). Another band assigned to bpy, found at 1470 for the guest **1**, shifts to 1465 cm^{-1} upon β-CD and TRIMEB encapsulation, whilst the remaining bpy bands remain mostly unshifted. These features are coherent with the partial inclusion of the bipyridine fragment proposed by us for adducts **2** and **3**.

In view of better understanding the behaviour of **1** in physiological media, in particular the Ru–Cl hydrolysis process and how it is affected by CD encapsulation, a Raman study was carried out for the solid samples **1**-**3** and their solutions, both in water and in physiological serum. The substitution of the chloride by a water molecule in the first coordination sphere of Ru(II) is an essential step in the activation of the drug *in vivo*, as the labile H_2O will subsequently leave the metal coordination environment enabling a covalent bond to be formed between the ion and DNA (possibly with one of the purine or pyrimidine bases), besides the probable intercalation of the bipyridine moiety.

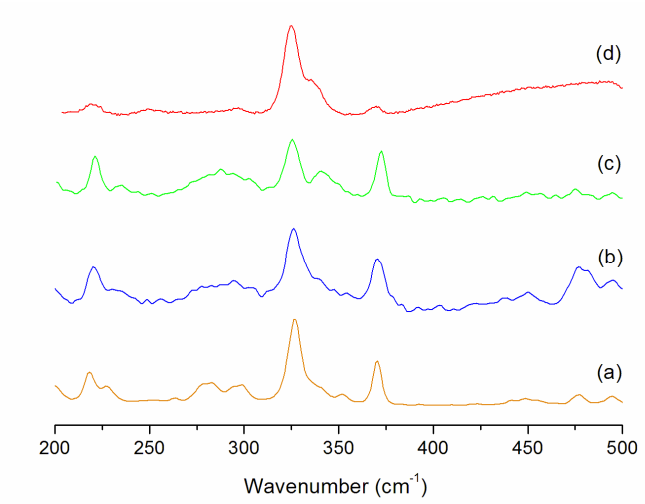

Figure 6 – Raman spectra of (a) solid [Ru([9]aneS$_3$])(bpy)Cl]Cl (**1**), (b) solid [Ru([9]aneS$_3$])(bpy)Cl]Cl·β-CD (**2**), (c) solid [Ru([9]aneS$_3$])(bpy)Cl]Cl·TRIMEB (**3**) and (d) a 10mM aqueous solution of **1**.

The Raman spectra for solid [Ru([9]aneS3])(bpy)Cl]Cl (**1**) at low wavenumber shows several bands associated with bpy and υ(Ru–N) modes (see Table 1 and Figures S3 and S4 in the Supplementary Material). These are practically unaffected by inclusion and are also quite stable in solution as they hardly suffer modifications by dissolving the samples **1**-**3** in water or serum. An exception is found for the band at 477 cm^{-1} (Figure 6), that reveals a shoulder in adducts **2** and **3** (see Table 1). In addition, the bands at 477 and 495 cm^{-1} feature a slight increase in intensity in the spectrum of solid **2** (but not in that of solid **3**).

Interestingly, the υ(Ru–Cl) stretching modes at 282 and 298 cm^{-1} for **1** are also affected by encapsulation in both hosts, appearing as broad bands centred around 294 for **2** and 288 cm^{-1} for **3**; this may reflect the more symmetric environment around the guest in the supramolecular adducts. Upon dissolution of compounds **1**-**3** the υ(Ru–Cl) weak bands disappear, either when using water or serum.

Table 1 – Selected vibrational modes for compounds **1**-**3**.

Selected bands (cm^{-1})				
1	**2**	**3**	**serum 8mM solution of 1**	Approximate description
282, 298	294	288	298	υ(Ru–Cl) *
326, 338 (sh)	326, 340 (sh)	326, 340	326, 338	υ(Ru–N)
371	371	372	—	υ(Ru–N) and υ(C–C) : bpy **
477	477, 482	477, 482	—	Ru–bipyridine ***

(*) By reference to the Mo–Cl mode reported for molybdenocene at 263 cm^{-1} [9].
(**) As calculated by Túlio E. Chavez-Gil et al. [44].
(***) By reference to a vibrational mode reported for $[Ru(bpy)_3]^{2+}$ by H. Riesen et al. [45].

These vibrational spectroscopic results suggest that in solution the interaction between the CD hosts and **1** remain somehow identical to that proposed in the solid state. The disappearance of the υ(Ru–Cl) bands is indicative of a complete hydrolysis of the chloride, even when $[Ru([9]aneS_3])(bpy)Cl]Cl$ is encapsulated in β-CD and TRIMEB (see Figures S3 and S4), which occurs promptly both in aqueous and in physiological media ($[Cl^-]$ = 0.9% *(w/v)*= 154 $mmol.dm^{-3}$).

4. Concluding Remarks

Inclusion compounds comprising cyclodextrins and the ruthenium(II) complex with the face capping ligand trithiacyclononane and with 2,2'-bipyridine have been prepared with a 1:1 host-to-guest stoichiometry, and characterised in the solid state by various techniques, including powder diffraction studies (XRD).

The low crystallinity of $[Ru([9]aneS_3])(bpy)Cl]Cl·β$-CD (**2**) prevented a complete structural description based on powder XRD. Nevertheless, the compound could be indexed with a typical monoclinic ($P2_1$) unit cell having dimensions slightly larger than those found for pure β-CD and similar to that of $[CuCl_2(H_2O)_2]·β$-CD [29]. Thus, it is proposed a partial inclusion of $[Ru([9]aneS_3])(bpy)Cl]Cl$ with its bulky part protruding from the CD cavity.

Monte Carlo structural optimisation using powder X-ray data of $[Ru([9]aneS_3])(bpy)Cl]Cl·$TRIMEB (**3**) allowed the calculation of a hypothetical structural model in which the cationic $[Ru([9]aneS_3])(bpy)Cl]^+$ guest complex is located mostly outside the TRIMEB cavity host (as also proposed for compound **2**), most likely due to its relatively large size. The orientation of TRIMEB molecules is typical, forming tilted channels running parallel to the *c*-axis of the unit cell.

FT-IR data further validate the proposed supramolecular interactions between the CDs and **1** as it points to partial inclusion of the bpy fragment in adducts **2** and **3**. TG shows good host-to-guest affinity in both compounds and $^{13}C\{^1H\}$ CP/MAS NMR depicts symmetrisation of the hosts and the guest carbon resonances as a result of their mutual interaction.

Raman studies on the hydrolysis of the Ru–Cl bond show that the two cyclodextrins are unable to

protect it: dissolution of either the complex [Ru([9]aneS3])(bpy)Cl]Cl (**1**) or the adducts **2** and **3** resulted in loss of the chlorine ligand. Improvement of the chemical design for these compounds is thus needed in order to avoid hydrolysis to take place before they reach its biological target, and thus hinder competition by other biomolecules (*e.g.* glutathione or albumin).

Furthermore, investigation about the effect of CD encapsulation on the cytotoxic activity of ruthenium(II) compounds with planar amines will be carried out. Molecular encapsulation of this class of complexes may be advantageous in several ways from a pharmaceutical point of view, such as enhancing the solubility of complexes in water, avoiding *in vivo* inactivation and reducing the cytotoxic effects towards healthy cells.

Electronic Supporting Information

Le Bail whole-powder-diffraction-pattern profile fittings in the monoclinic $P2_1$ space group for compounds [Ru([9]aneS$_3$])(bpy)Cl]Cl·β-CD (**2**) and [Ru([9]aneS$_3$])(bpy)Cl]Cl·TRIMEB (**3**). Table with the fractional atomic coordinates (as supplied by FOX) and CIF file with the optimised structural model of [Ru([9]aneS$_3$])(bpy)Cl]Cl·TRIMEB. Raman spectra of serum 8mM solutions of [Ru([9]aneS$_3$])(bpy)Cl]Cl (**1**) and **2** compared with the spectrum of solid **2**, and of serum solutions of **1** (8mM) and **3** (10mM) compared with the spectrum of solid **3**.

Acknowledgements

This work was partly funded by the FCT, POCI and FEDER (Project POCI/SAU/BEB/66869/2006). We wish to thank Prof. João Rocha for access to research facilities.

References

[1] J. Szejtli, *Chem. Rev.* **98** (1998), pp. 1743-1753.

[2] W. Saenger, *Angew. Chem. Int. Edit. Engl.* **19** (1980), pp. 344-362.

[3] E.M.M. Del Valle, *Process Biochem.* **39** (2004), pp. 1033-1046.

[4] W. Sliwa, T. Girek, *Heterocycles* **60** (2003), pp. 2147-2183.

[5] E. Fenyvesi, L. Szente, N.R. Russel. In *Comprehensive Supramolecular Chemistry;* Szejtli, J.; Osa, T. Eds.; Pergamon: Oxford, 1996; *3*; pp. 305-366.

[6] H.M. Colquhoun, J.F. Stoddart, D.J. Williams, *Angew. Chem. Int. Edit. Engl.* **25** (1986), pp. 487-507.

[7] Z. Petrovski, M.R.P. Norton de Matos, S.S. Braga, C.C.L. Pereira, M.L. Matos, I.S. Gonçalves, M. Pillinger, P.M. Alves, C.C. Romão, *J. Organomet. Chem.* **693** (2008), pp. 675-684.

[8] C.C.L. Pereira, M. Nolasco, S.S. Braga, F.A. Almeida Paz, P. Ribeiro-Claro, M. Pillinger, I.S. Gonçalves, *Organometallics* **26** (2007), pp. 4220-4228.

[9] S.S. Braga, M.P.M. Marques, J.B. Sousa, M. Pillinger, J.J.C. Teixeira-Dias, I.S. Gonçalves, *J. Organomet. Chem.* **690** (2005), pp. 2905-2912.

[10] S.S. Braga, I.S. Gonçalves, M. Pillinger, P. Ribeiro-Claro, J.J.C. Teixeira-Dias, *J. Organomet. Chem.* **632** (2001), pp. 11-16.

[11] S.S. Balula, A.C. Coelho, S.S. Braga, A. Hazell, A.A. Valente, M. Pillinger, J.D. Seixas, C.C. Romão, I.S. Gonçalves, *Organometallics* **26** (2007), pp. 6857-6863.

[12] S.S. Braga, F.A.A. Paz, M. Pillinger, J.D. Seixas, C.C. Romão, I.S. Gonçalves, *Eur. J. Inorg. Chem.* (2006), pp. 1662-1669.

[13] S.S. Braga, I.S. Gonçalves, P. Ribeiro-Claro, A.D. Lopes, M. Pillinger, J.J.C. Teixeira-Dias, J. Rocha, C.C. Romão, *Supramol. Chem.* **14** (2002), pp. 359-366.

[14] S.S. Braga, I.S. Gonçalves, A.D. Lopes, M. Pillinger, J. Rocha, C.C. Romão, J.J.C. Teixeira-Dias, *Dalton Trans.* (2000), pp. 2964-2968.

[15] C.C.L. Pereira, S.S. Braga, F.A.A. Paz, M. Pillinger, J. Klinowski, I.S. Gonçalves, *Eur. J. Inorg. Chem.* (2006), pp. 4278-4288.

[16] S.S. Braga, S. Gago, J.D. Seixas, A.A. Valente, M. Pillinger, T.M. Santos, I.S. Gonçalves, C.C. Romão, *Inorg. Chim. Acta* **359** (2006), pp. 4757-4764.

[17] J. Madureira, T.M. Santos, B.J. Goodfellow, M. Lucena, J.L.P. de Jesus, M.G. Santana-Marques, M.G.B. Drew, V. Félix, *Dalton Trans.* (2000), pp. 4422-4431.

[18] T.M. Santos, J. Madureira, B.J. Goodfellow, M.G.B. Drew, J. Pedrosa de Jesus, V. Félix, *Met.-Based Drugs* **8** (2001), pp. 125-135.

[19] B.J. Goodfellow, V. Félix, S.M.D. Pacheco, J.P. deJesus, M.G.B. Drew, *Polyhedron* **16** (1997), pp. 393-401.

[20] Ž. Petrovski, S.S. Braga, A.M. Santos, S.S. Rodrigues, I.S. Gonçalves, M. Pillinger, F.E. Kühn, C.C. Romão, *Inorg. Chim. Acta* **358** (2005), pp. 981-988.

[21] Ž. Petrovski, S.S. Braga, S.S. Rodrigues, C.C.L. Pereira, I.S. Gonçalves, M. Pillinger, C. Freire, C.C. Romão, *New J. Chem.* **29** (2005), pp. 347-354.

[22] A. Boultif, D. Louer, *J. Appl. Crystallogr.* **37** (2004), pp. 724-731.

[23] J. Rodriguez-Carvajal, *FULLPROF - A Program for Rietveld Refinement and Pattern Matching Analysis, Abstract of the Satellite Meeting on Powder Diffraction of the XV Congress of the IUCR, Toulouse, France, 1990, p.127.*

[24] T. Roisnel, J. Rodriguez-Carvajal, *WinPLOTR [June 2005] - A Windows Tool for Powder Diffraction Pattern Analysis. Materials Science Forum, Proceedings of the Seventh European Powder Diffraction Conference (EPDIC 7), 2000, p.118-123, Ed. R. Delhez and E.J. Mittenmeijer.*

[25] J. Laugier, B. Bochu, *CHECKCELL - A Software Performing Automatic Cell/Space Group Determination, Collaborative Computational Project Number 14 (CCP14), Laboratoire des Matériaux et du Génie Physique de l'Ecole Supérieure de Physique de Grenoble (INPG), France, 2000* .

[26] A. LeBail, H. Duroy, J.L. Fourquet, *Mater. Res. Bull.* **23** (1988), pp. 447-452.

[27] A. Boultif, D. Louer, *J. Appl. Crystallogr.* **24** (1991), pp. 987-993.

[28] D. Louer. In *Automatic Indexing: Procedures and Applications, Accuracy in Powder Diffraction II*: Gaithersburg, MD, USA, 1992 pp. 92-104.

[29] G. Kurokawa, M. Sekii, T. Ishida, T. Nogami, *Supramol. Chem.* **16** (2004), pp. 381-384.

[30] P.E. Werner, L. Eriksson, M. Westdahl, *J. Appl. Crystallogr.* **18** (1985), pp. 367-370.

[31] F.H. Allen, *Acta Cryst. B* **58** (2002), pp. 380-388.

[32] F.H. Allen, W.D.S. Motherwell, *Acta Cryst. B* **58** (2002), pp. 407-422.

[33] V. Favre-Nicolin, R. Cerny, *FOX - A Program for ab initio Structure Solution from Powder Diffraction Data, Program Developed for the Swiss National Science Foundation, University of Geneva, Geneva, Switzerland, 2000* pp.

[34] V. Favre-Nicolin, R. Cerny, *J. Appl. Crystallogr.* **35** (2002), pp. 734-743.

[35] B. Serli, E. Zangrando, T. Gianferrara, C. Scolaro, P.J. Dyson, A. Bergamo, E. Alessio, *Eur. J. Inorg. Chem.* (2005), pp. 3423-3434.

[36] P. Walters, M. Stahl, *BABEL Version 1.3 - A Program for the Interconversion of File Formats Used in Molecular Modelling, Department of Chemistry, University of Arizona, Tucson, AZ 85721, US, 1996* pp.

[37] K. Harata, *Bull. Chem. Soc. Jpn.* **61** (1988), pp. 1939-1944.

[38] A. Harada, K. Saeki, S. Takahashi, *Organometallics* **8** (1989), pp. 730-733.

[39] S.S. Braga *et al.*, *(In Preparation)* .

[40] S.J. Heyes, N.J. Clayden, C.M. Dobson, *Carbohydr. Res.* **233** (1992), pp. 1-14.

[41] M.J. Gidley, S.M. Bociek, *J. Am. Chem. Soc.* **110** (1988), pp. 3820-3829.

[42] R.P. Veregin, C.A. Fyfe, R.H. Marchessault, M.G. Taylor, *Carbohydr. Res.* **160** (1987), pp. 41-56.

[43] M.R. Caira, S.A. Bourne, W.T. Mhlongo, P.M. Dean, *Chem. Commun.* (2004), pp. 2216-2217.

[44] T.E. Chavez-Gil, D.L.A. de Faria, H.E. Toma, *Vib. Spectrosc.* **16** (1998), pp. 89-92.

[45] H. Riesen, L. Wallace, E. Krausz, *Chem. Phys.* **198** (1995), pp. 269-280.

Graphical abstract

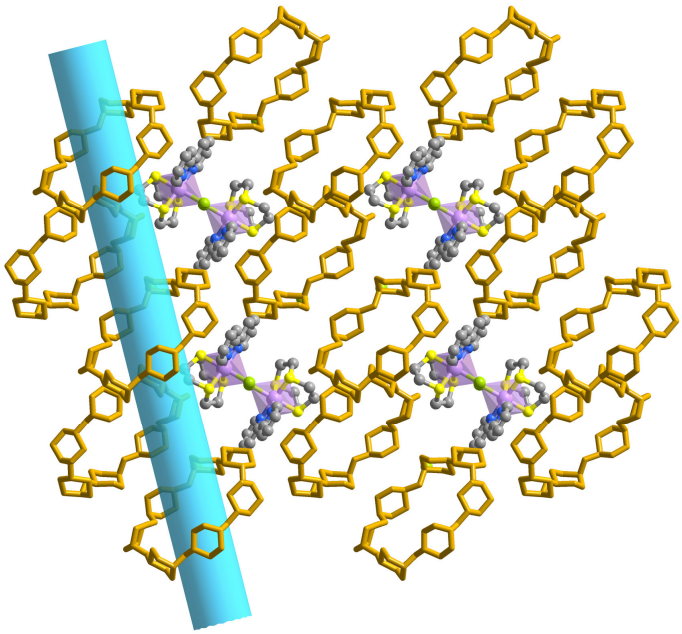

[Ru([9]aneS$_3$)(bpy)Cl]Cl was immobilised in β-CD and TRIMEB yielding two crystalline 1:1 adducts studied by powder XRD, TGA, $^{13}C\{^1H\}$ CP/MAS NMR, FT-IR and Raman. For [Ru([9]aneS$_3$)(bpy)Cl]Cl·TRIMEB a channel packing mode is proposed, obtained by Monte Carlo optimisation of the XRD data.